



Published in final edited form as:

*Leuk Lymphoma*. 2006 November ; 47(11): 2388–2399.

## Characterization of antibody-containing vesicles shed from B-lymphoma cell lines: exposure of annexin V binding sites

Rosana B. Michel<sup>1</sup>, Mones Abu-Asab<sup>2</sup>, Maria Tsokos<sup>2</sup>, and M. Jules Mattes<sup>1</sup>

<sup>1</sup>Center for Molecular Medicine and Immunology, Belleville, NJ

<sup>2</sup>Laboratory of Pathology, National Institutes of Health, Bethesda, MD, USA

### Abstract

Antibodies (Abs) to CD20 or HLA-DR, after binding to the B-lymphoma cell line RL following an overnight incubation at 37°C, accumulate in the form of shed vesicles, which develop in the center of the cell clusters that are spontaneously formed by this cell line. These vesicles coalesce into fairly stable large structures, which we refer to as conglomerates of shed vesicles (CSVs). In the present study, we have extended our previous investigations into the nature of this material. Electron microscopy revealed a conglomerate of heterogeneous vesicles, which looked like pinched-off cytoplasmic projections. CSVs developed similarly either with or without Ab, demonstrating that CSV production is a spontaneous process that incorporates bound Abs if they are present. Before delivery to CSVs, the Abs capped on the cell surface. CSVs had high expression of annexin V binding sites, which are phagocytic signals that are exposed on damaged cells. For CSVs that were cell bound, which are frequently observed, the annexin V binding sites were only in the CSVs, and not on the surface of the intact cell. Although all CSVs contained both Abs and annexin V binding sites, the precise distribution of these two ligands was generally different. Annexin V binding sites were present on caps as well as on CSVs, and appear as soon as caps are formed. In cells incubated with anti-HLA-DR, CD20 was delivered to the CSVs together with HLA-DR, suggesting an association between these two molecules. CSVs prepared with anti-HLA-DR, but not CSVs prepared with anti-CD20, contained considerable numbers of nuclear fragments, identified by propidium iodide staining.

### Keywords

B-cell lymphoma; antibody therapy; CD20; HLA-DR; antibody shedding; annexin V

### Introduction

We previously described a novel shedding process occurring after the binding of certain antibodies (Abs) to some B-lymphoma cell lines: the Abs accumulated in relatively large cytoplasmic fragments (CFs) that were shed from the cell surface, presumably by a pinching-off process [1]. With antibodies to CD20 or HLA-DR, but not with Abs to other cell surface

---

Correspondence: M. Jules Mattes, Center for Molecular Medicine and Immunology, 520 Belleville Avenue, Belleville, NJ 07109, USA. E-mail: mjmmattes@gscancer.org.

**Publisher's Disclaimer:** Full terms and conditions of use: <http://www.informaworld.com/terms-and-conditions-of-access.pdf>

This article may be used for research, teaching and private study purposes. Any substantial or systematic reproduction, re-distribution, re-selling, loan or sub-licensing, systematic supply or distribution in any form to anyone is expressly forbidden.

The publisher does not give any warranty express or implied or make any representation that the contents will be complete or accurate or up to date. The accuracy of any instructions, formulae and drug doses should be independently verified with primary sources. The publisher shall not be liable for any loss, actions, claims, proceedings, demand or costs or damages whatsoever or howsoever caused arising directly or indirectly in connection with or arising out of the use of this material.

antigens, the great majority of bound Ab accumulated in these CFs within 1 day after Ab binding. This process, if it occurs in natural tumors, would probably affect the therapeutic results obtained with these Abs, which are in clinical use [2,3]. Chronic lymphocytic leukemia patients treated with rituximab were found to have 'debris' circulating in the blood, often attached to viable cells, which contained a large amount of the Ab injected [4], and which was similar in many respects to the CFs, as we have discussed previously [1]. The CFs form large, heterogeneous structures that often appear to be composed, in part, of smaller vesicles. Therefore, to better describe the objects observed, we have altered our previous nomenclature: the term CF is now reserved for single, small vesicles, and the much larger, more complex objects are now referred to as conglomerates of shed vesicles (CSVs). This term is intended to be merely descriptive, and a better name for these objects will be possible when their nature is better understood. A budding vesicle that is not yet detached from the cell will be referred to as a bleb. In some respects, single CFs resemble the lymphoglandular bodies that have been described by pathologists for many years [1,5], which are useful in the diagnosis of B-cell lymphoma. CFs developed in the center of large clusters of cells, so they may be formed by the combined secretions of all of the surrounding cells, which would explain their large size and their low abundance in comparison to the number of cells. The cell line that produced CFs most abundantly was RL, a diffuse large-cell B-lymphoma, but they were also produced by Raji cells, and, in total, by five of seven B-lymphoma cell lines tested, but they were not produced by lymphoblastoid cell lines (transformed by EB virus) treated in the same way.

In the present study, we have continued our investigation into the nature of this shed material to better understand its structure and function. Immunofluorescence experiments were performed with Alexa-488-anti-HLA-DR, to extend the previous studies with Alexa-488-anti-CD20. CSVs prepared with anti-HLA-DR contained the CD20 antigen, as well as the antigen recognized. Annexin V binding sites, which are normally sequestered on the inner face of the plasma membrane [6], were highly expressed in CSVs, although generally in a location separate from the location of the Abs. Both Abs that are delivered to CSVs form caps on the cell surface 1 – 3 h after Ab binding, which is long before large CSVs are produced, suggesting that the caps are delivered to CSVs. Caps induced by anti-CD20, even those of smallest size, were also stained by annexin V. CSVs prepared with anti-HLA-DR, but not those prepared with anti-CD20, were found to contain abundant nuclear fragments (stained by propidium iodide). Electron microscopy demonstrated that CSVs were produced in the absence of Ab, as well as in the presence of Ab, in the center of the clusters that form spontaneously with these cell lines. That is, if Abs are present, they are delivered to the CSVs which are spontaneously produced.

## Materials and methods

### Cell lines, Abs and Ab conjugates

The RL cell line, a diffuse, large cell B-lymphoma, was described previously [7], and is available from the American Type Culture Collection (ATCC, Manassas, VA, USA). Cells were cultured as described [7,8]. They were tested routinely for mycoplasma by the Mycotect assay (Life Technologies, Grand Island, NY, USA), and were negative. All of the Abs used were described previously [7,8]. Anti-CD20 Ab (1F5) and anti-HLA-DR Ab (L243) were produced by hybridomas obtained from ATCC. The Ab subclass is IgG2a for both. A control Ab of the same subclass was also tested, namely the IgG2a Ab MX352a. Rabbit anti-human IgM was purchased from DAKO Corp. (#A425, IgG fraction; Carpinteria, CA, USA). Anti-CD20 Abs, L243 and the control Ab were conjugated to Alexa-488 (Molecular Probes, Eugene, OR, USA) as described previously [9]. Abs were sterilized by passage through a 0.2 µm pore size filter. Rabbit antibodies to human IgG+IgM (heavy and light chains) were obtained from Jackson ImmunoResearch (#309-0056-044; West Grove, PA, USA), and fluorescein-

conjugated donkey antibodies to rabbit IgG were obtained from Pierce Chemicals (#31571; Rockford, IL, USA).

### Immunofluorescence

Except as noted, fluorescent CSVs were generated by incubating cells overnight at 37°C in standard tissue culture medium in an atmosphere of 5% CO<sub>2</sub>, supplemented with Ab at 10 µg/ml. The Ab was added in 5 µl to 2.5 × 10<sup>5</sup> cells in a well of a 24-well plate, in 0.5 ml of medium. After the incubation, cells were transferred into 15-ml tubes and washed twice with 5 ml of medium. For the last wash, medium without phenol red was used. After the final wash, the cells were resuspended in 100 µl and examined in a slide chamber made with a cover slip adhered to two strips of double-sided tape. Except when red fluorescent reagents were used, the final buffer contained 1 µg/ml propidium iodide, to identify dead cells. To examine intact clusters, cells were transferred directly to slides from the 24-well plate, without washing, as gently as possible. In some experiments, after preparation of CSVs with an unconjugated Ab, the cells were stained with an Alexa-488-conjugate of another Ab for 1 h at 12°C (maintained with a Boekel MiniFridge II, Feasterville, PA, USA), also at 10 µg/ml. Alternatively, cells were stained for 45 min at room temperature with Alexa-488- or Alexa-568-annexin V by addition of 5 µl of the reagent (Molecular Probes) to the pelleted cells resuspended in the residual volume (approximately 130 µl). The buffer used for annexin V staining (and for the washes used before staining) was complete tissue culture medium supplemented with 2 mM CaCl<sub>2</sub>, without phenol red. To induce capping of surface IgM on RL cells, cells were incubated for 1 h on ice with rabbit anti-human IgM at 20 µg/ml, then washed and incubated similarly with fluorescein-conjugated donkey anti-rabbit IgG. After washing at room temperature, cells were incubated with Alexa-568-annexin for 45 min at 37°C. Cells were examined under a fluorescence microscope, as described previously [9], and photographs were taken with a digital camera.

### Electron microscopy

Intact clusters of RL cells, prepared with or without Alexa-488-1F5, were examined; these two types of clusters were similar in size. After the overnight incubation, in a total volume of 0.5 ml, 0.35 ml of supernatant was gently removed, leaving the cells in the well. To each well, 1.85 ml of 2.5% glutaraldehyde (EM grade, Sigma Chemicals, St Louis, MO, USA) was gently added in 0.1 M sodium cacodylate buffer, pH 7.2, with 5 mM CaCl<sub>2</sub>. After 2 h at 37°C, the cells were gently transferred to a tube containing 12 ml of the fixative, and the incubation continued overnight at 4°C. The size and general appearance of the clusters was not affected by the fixation, and the fluorescence of the Ab was still clearly seen in the fixed clusters, despite the weak autofluorescence of the fixed cells. The cells were suspended in 1.5% low-melting-point agarose, to maintain the natural clusters. The hardened agarose was double-fixed with 0.5% osmium tetroxide, dehydrated, and embedded into Spurr's epoxy resin. Ultrathin sections (90 nm) were double-stained with uranyl acetate and lead citrate, and viewed under a transmission electron microscope.

## Results

### Appearance of CSVs by phase contrast microscopy

We previously showed the appearance of CSVs after staining with Wright's stain, in air-dried cell preparations. Such samples reveal the morphology in great detail but, in practice, CSVs are more readily observed by phase contrast observation of cells in suspension. Figure 1 shows the appearance of such samples. RL cells were incubated overnight with Alexa-488-1F5, then washed, and CSVs were identified by their bright fluorescence, as also shown previously [1]. CSVs appear to consist of conglomerates of heterogeneous objects, including vesicles and granular material, irregular in shape and heterogeneous in size. Most of the CSVs shown in

Figure 1 are relatively large, but CSVs varied greatly in size, and many were smaller. CSVs bound to a single cell are common (Figure 1E,F). It is also common to see clusters of two to three cells, with CSVs between the cells. When interpreting these photographs, it should be emphasized that RL cells, similar to many B-lymphoma cells lines and B-lymphoblastoid cell lines, normally grow as large clusters of 5 – 15 cells, and the CSVs develop in the center of the clusters (suggesting that many surrounding cells may contribute to the formation of the CSVs). This was shown previously with 1F5 [1], and similar results with L243 are also shown in Figure 2. In this experiment, cells were examined without washing, and were transferred directly to slides, as gently as possible, to keep the clusters intact. Because the staining is so bright, the presence of unbound fluorescent Ab in the medium does not interfere with observation. We note that washing the cells, as normally performed, causes almost all of the cell clusters to be dispersed.

### Electron microscopy

Intact clusters were embedded in agarose and examined as described in Materials and Methods. In the center of the clusters, there was a heterogeneous mass of small vesicles, between the cells (Figure 3). These vesicles appeared to contain primarily normal cytoplasmic constituents, with relatively few organelles, as indicated in Figure 3 (D). Nuclear fragments were not observed. Signs of apoptosis (condensed nuclear and cytoplasmic material) or necrosis (oedematous dissolution of organelles) were not observed in either the CSVs or in the adjacent cells. Adjacent cells frequently had cytoplasmic projections, which appear to be the likely source of the vesicles via a pinching-off process. Clusters occurring after 1F5 treatment (Figure 3C,D) or in the absence of Abs (Figure 3A,B) had similar vesicles in the center, indicating that vesicle formation itself was not dependent on the presence of Ab, but the vesicles appeared to be more extensively formed in the presence of Ab, meaning that the space between cells in the center of the clusters was almost entirely filled with the vesicles.

### Abs form caps before production of CSVs

Large fluorescent CSVs do not appear until after an overnight incubation with Ab. Thus, we looked at early time points (1 – 3 h) to determine the initial events that occur. Using Alexa-488-anti-CD20, with a 37°C incubation, capping of the Ab was found to occur rapidly: within 1 h, the majority of the cells were capped (Figure 4), meaning that much of the fluorescence was concentrated to a small spot on the cell surface. Capping was abolished by low temperatures, of either 0 – 4°C or 12°C, but it was not inhibited by 10 mM NaN<sub>3</sub>. In cells stained at low temperatures, a small number of cells (<10%) were still capped; it is likely that such capping was present before the Ab was added, but there is no direct evidence to support this. In any case, staining at 12°C resulted in a ringed staining pattern for more than 90% of the cells, with some patchiness of the fluorescence. Most of the capped cells, after incubation at 37°C, also had relatively faint ringed staining, indicating that not all of the bound Ab was delivered to the cap (Figure 4A). By 2 – 3 h, in addition to caps, small blebs were detected, which are likely to be related to the development of CSVs. Many of the blebs were associated with bright fluorescence, although staining was not on the surface of the bleb, but rather appeared to be granular, sometimes adjacent to the bleb, or at the ‘base’ of the bleb (where it was conjoined with the cell surface) (Figure 4B – D). Thus, it appeared that blebs sometimes developed adjacent to the caps. However, a considerable number of blebs were unstained, presumably unrelated to the capping of 1F5. Small fluorescent CSVs (separated from cells) also became evident after approximately 1 h. Experiments with Alexa-488-L243 produced results generally similar to those obtained with Alexa-488-1F5, with ringed staining changing to caps over a period of 1 – 3 h. An overnight incubation with Alexa-488-L243 produced fluorescent CSVs that were generally very similar to those produced with Alexa-488-1F5, but CSVs prepared with L243 were somewhat larger and more abundant. Also, L243 stained prominent small

cytoplasmic vesicles (in addition to the staining of CSVs and the cell surface), which were much less prominent after staining with 1F5.

### **Fluorescent CSVs prepared with anti-HLA-DR (L243) also contain CD20**

Because fluorescent CSVs were induced by both 1F5 and L243, we considered the possibility that CSVs prepared with one of the Abs might also contain the second antigen. CSVs were prepared by overnight incubation with unconjugated L243, and the cells were then stained for 1 h at 12°C with Alexa-488-anti-CD20. The low temperature was used to insure that the 1F5 Ab did not affect antigen distribution (but essentially identical results were obtained if this incubation was performed at 37°C). The CSVs, which were readily identified by phase contrast observation, were all stained brightly by anti-CD20 (Figure 5). This staining was antigen specific, because non-reactive Abs conjugated with Alexa-488 in the same way produced no nonspecific staining. Cell preparations that had been incubated overnight with L243 had a relatively large number of small clusters of two to three cells; these were not as common after overnight incubation with 1F5, and we attribute this to the fact that L243 tends to aggregate cells to a greater extent than 1F5. The staining of the CSVs in these experiments appeared to be just as bright as when the cells were incubated overnight at 37°C with Alexa-488-1F5. We conclude that CD20 is delivered to CSVs in the absence of an anti-CD20 Ab, presumably due to binding of the anti-HLA-DR Abs. However, not all of the CD20 on the cell surface was transported to the CSVs in these experiments. Most of the cells had a ringed staining pattern, and some had a capped staining pattern. In representative experiments of 150 cells counted, 67% had a ringed pattern, 20% had a cap, and 13% were unstained (some of the unstained cells may have had all of the CD20 antigen stripped from the surface). For this count, a cell was considered to be capped if less than half of the cell surface was stained but, in almost all cases, the cap was much smaller than this. The cells having a bound CSV were no less likely than other cells to have ringed staining. As a control, untreated cells were stained similarly with Alexa-488-1F5, for 1 h at 12°C. As expected, no fluorescent CSVs were present in this case. The membrane staining appeared to be brighter than in the samples pre-treated with L243, yet the difference was not dramatic. Thus, it appears that only a fraction of the CD20 antigen was delivered to CSVs by L243. Alternatively, CD20 molecules that were stripped from the cell surface may have been replaced by new CD20 molecules. When this experiment was performed in the inverse order, using overnight incubation with unconjugated 1F5 followed by a 1-h incubation with Alexa-488-L243, the results were similar in that the CSVs induced contained abundant HLA-DR antigen. However, cell surface staining with L243 remained bright, suggesting that only a small fraction of the total HLA-DR antigen was delivered to CSVs by 1F5.

### **The presence of nuclear fragments within fluorescent CSVs prepared with L243**

In most experiments in which only green conjugates were used, the final samples contained propidium iodide, which stains DNA red. CSVs prepared with L243 were found to contain a considerable number of red fluorescent spots, which are assumed to be nuclear fragments (Figure 6). Although these fragments were clearly stained red by PI, the staining was relatively weak, much less bright than the staining of the few dead cells that were present in these samples. CSVs prepared with 1F5 contained few nuclear fragments, and most of the CSVs prepared with 1F5 did not contain any nuclear fragments. Therefore, the presence of nuclear fragments is not inherent to the process of CSV formation. Our observations strongly suggest that fluorescent CSVs prepared with 1F5 are produced by viable cells, but the results with L243 are more difficult to interpret definitively, due to the presence of these nuclear fragments. That is, CSVs containing nuclear fragments are similar in some respects to apoptotic cells or clusters of apoptotic bodies. It should be noted that, in the present experiments, incubating cells overnight with 1F5 or L243 at 10 µg/ml, produced little if any evident toxicity, as determined by viability counts (data not shown). Moreover, long-term viability was determined by

counting cells until they multiplied 16-fold: 1F5 had no effect on the growth rate of RL cells (data not shown). Considering the great similarity of CSVs containing 1F5 or L243, it is most likely that the CSVs containing L243 also are produced by viable cells. The frequent presence of nuclear fragments in fluorescent CSVs prepared with L243 may be related to the fact that L243 has been reported to induce toxicity, via caspase-independent apoptosis, in most B-lymphoma cell lines [10,11]. As noted above, there was no significant amount of cell death in our experiments, but there may have been a low level of cell death, and one dead cell could generate a large number of small nuclear fragments. Nagy et al. [10,11] described the rapid disintegration of dead cells induced by L243 binding, within 30 min, which might result in some residual nuclear fragments.

### Reactivity of annexin V with CSVs and other objects

The phospholipids that react with annexin V are primarily on the inner face of the cell membrane in normal cells, and move to the exposed outer face only under certain conditions, such as apoptosis. These lipids include phosphatidyl serine (PS), phosphatidyl ethanolamine, and phosphatidyl inositol, but the major ligand is considered to be PS [6]. When CSVs were prepared with either 1F5 or L243, they reacted strongly with annexin V (Figure 7). CSVs attached to the surface of a cell reacted strongly whereas the rest of the cell surface was totally non-reactive. The pattern of staining of the CSVs was complex: there was some granular material but, in addition, there were frequently smaller vesicles within the CSVs that had sharp, bright, membrane staining (Figure 7B,H). Double-staining with annexin V and 1F5 (Figure 7E,F,H), using an overnight incubation at 37°C with 1F5 followed by a 45-min incubation with annexin V at room temperature, demonstrated that there was some overlap but that, in general, different structures were stained, although both were present in the same CSVs. In some cases, objects stained by annexin V were largely separate from the objects stained with 1F5 (Figure 7H) but, in other cases, they were closely apposed, or partially superimposed (Figure 7E,F). To examine smaller CSVs, a shorter 1F5 incubation of only 3 h was used. At this time point, only a few small CSVs were present, and most cells were capped, as described above. Annexin V stained all of the small CSVs brightly and, in addition, stained all of the caps (Figure 8). The only cells that were unstained by annexin V were the ringed cells. Even the smallest caps had some red staining (Figure 8). Thus, annexin V binding sites appear as soon as caps are formed. Again, annexin staining was generally separate from the 1F5 staining, even in the small caps, as if different objects within the same cap were stained. In these capped cells, annexin V staining was typically in the form of small spots (which could be small vesicles). To determine whether caps induced with other Abs would also express annexin V binding sites, surface IgM on RL cells was capped with rabbit anti-human IgM and fluorescein-conjugated donkey anti-rabbit IgG. After 45 min at 37°C, the anti-Ig Abs formed caps in most of the cells, but there was no staining of the caps or the ringed cells by Alexa-568-annexin (data not shown).

In addition to CSVs, annexin V also stained other objects in these preparations, all of which were seen equivalently in both control samples (incubated in medium) and in samples that had been incubated with Abs. Three types of objects were stained (Figure 9). First, although the great majority of viable cells were unstained by annexin V, a small fraction (<2%) had bright membrane staining. These cells presumably are the apoptotic cells, and almost all looked abnormal by phase contrast observation (Figure 9C – E). Second, dead cells, as identified by propidium iodide staining, were also stained brightly by annexin V (Figure 9F – H). Third, small vesicles had membrane staining (Figure 9A – B). These vesicles ranged in size from 1.0 – 6.6 µm in diameter, with a mean±SD of 4.3 ± 1.3 µm. Most (approximately 90%) were dark by phase contrast observation, but the remainder were refractile. There were also a considerable number of similar vesicles (by visible light) that were not stained with annexin V, and there was no evident morphological difference between the vesicles that were positive or negative for annexin V staining. These vesicles were all single (unclustered), and it is important to

emphasize that they were present, and similar in all respects, in both control and Ab-treated samples. Untreated samples of RL cells were double-stained with Alexa-488-1F5 and Alexa-568-annexin V, to determine whether the annexin-positive vesicles would stain with 1F5. Some of the vesicles were stained by 1F5, but the majority were unstained, and those that were stained had an intensity that was similar to that on the surface of viable cells. Thus, CD20 was sometimes present on these vesicles, but was not enriched in them.

## Discussion

The optimal nomenclature for the structures described here is uncertain, and may be better decided when their function is known. However, some tentative nomenclature is required. Given the heterogeneous structure revealed by visible light and electron microscopy, and the complex and heterogeneous staining pattern obtained with 1F5, L243 or annexin V, the term 'conglomerate of shed vesicles' appears to be appropriate, and better than the term 'cytoplasmic fragment', which we used previously [1]. Single vesicles can still be described as CFs. Other types of shed membranous material have been described previously, and given various names (as previously discussed in some detail [1]), but CSVs, as described in the present study, have not been reported. Cytoplasmic fragments have sometimes been described as 'blebs', but this term is too poorly defined, and has been applied to too many different structures to be useful in this case. Some blebs are temporary protrusions from the cell surface, but we would emphasize that CSVs become separated from the cell, presumably by a pinching-off process. Exosomes [12] are another type of vesicle that is shed from cells, but these arise from intracellular multivesicular bodies; thus, the mode of formation is distinct from a pinching-off process, and exosomes are much smaller than CSVs. In the early studies of Ab capping on the lymphocyte cell surface, shedding was routinely stated to be an alternative fate of the cap, but internalization was the major pathway [13,14] and structures similar to CSVs were not described. Moreover, these early studies utilized primarily Abs to surface Ig, which were not delivered to CSVs in our experiments [1].

The capping of 1F5 is clearly related to the development of CSVs. Despite extensive studies over many years with anti-CD20 Abs, there is little mention of capping with these Abs, although there is one previous report consistent with our observations [15]. Most of the capped cells also had fainter ringed staining, suggesting that the delivery of the Ab to caps was not efficient, in contrast to the capping induced by Abs to certain other antigens, particularly surface Ig. It should be noted that such results may depend on the particular cell line used, as well as on the particular Ab. The fact that CD20 was efficiently delivered to CSVs by L243, and HLA-DR antigen was delivered to CSVs by 1F5, can be attributed to the known association of the two proteins recognized [16].

The present study has revealed a number of new characteristics of CSVs. Electron microscopy demonstrated that CSVs were produced in the absence of Ab, as well as in the presence of Ab. Thus, delivery of bound Ab to CSVs represents incorporation into spontaneously shed vesicles. This observation appears to conflict with our previous finding, based on staining of cell smears with Wright's stain, that CSVs were not seen in the absence of Ab incubation [1]. However, this can be explained by proposing that large CSVs are stabilized by Ab binding, due to cross-linking and that, in the absence of Ab, the CSVs are dispersed into single small vesicles by normal handling methods. Such small vesicles would be easily overlooked in the absence of fluorescent staining, and might also be lost in the standard washing procedures used. Although CSVs were produced in the absence of Ab, it should be noted that there appeared to be more extensive production in the presence of the Ab 1F5, as indicated by the space between cells, in the center of the clusters, being entirely filled with vesicles. Thus, vesicle production may be enhanced by Ab binding; but the assays that have been used for detection of CSVs are not

quantitative, and further work is required to better estimate the number and size of vesicles produced.

The presence of annexin V binding sites within CSVs is a key observation. Annexin V stained CSVs brightly, whereas the cells to which CSVs were (sometimes) bound were otherwise totally negative. The annexin V sites detected in the present experiments may be on either the inner or the outer face of the membrane because the shed vesicles may not have an intact membrane. However, it is likely that PS asymmetry would be lost in either permeable or impermeable vesicles because phospholipid asymmetry is maintained by an energy-dependent enzyme [17]. Even the smallest cap of CD20 on the cell surface was stained by annexin V, as shown in our 3-h capping experiments. Therefore, it appears that either submicroscopic vesicles containing capped material are pinched off, or annexin V-binding sites may be exposed within the region of the cap, which would appear to require some type of membrane compartmentalization. Electron microscopy may be useful to resolve this question. A compartmentalized distribution of annexin V binding sites on the surface of viable cells has not been previously described, with the exception of a report by Dillon et al. [18], which is discussed in some detail below. Cocca et al. [19] demonstrated that an Ab to anionic phospholipids reacted primarily with the blebs of apoptotic Jurkat T leukemia cells, while annexin V reacted homogeneously with the cell surface. These data support the general idea of membrane compartmentalization of phospholipids, although not of annexin V binding sites in particular.

Apoptotic vesicles (apoptosomes) are known to express annexin V binding sites, but there are few reports of annexin V-stained vesicles produced by viable cells. One example is the work of Ran et al. [6], who reported the generation of annexin V-positive vesicles from viable endothelial cells. In their system, such vesicles were induced by oxidative stress or other inducing agents. They were produced by blood vessels within tumors but not by blood vessels in normal tissues, due evidently to some type of inductive signal in the tumor. Heijnen et al. [20] demonstrated that microvesicles shed from activated platelets have exposed annexin V binding sites, but such sites are also present on intact activated platelets (although not on normal platelets); thus, the situation is different from that described in the present study. Dillon et al. [18] reported that annexin V binding sites were exposed on the surface of normal B cells from the mouse spleen and bone marrow. These sites were normally distributed uniformly on the cell surface, but they co-capped with anti-IgM Abs. However, such spontaneous expression of annexin V binding sites has not been reported on human B-cells or B-lymphoma cell lines. The fact that annexin V staining has been used as a marker for apoptosis with human B-lymphoma cell lines [21,22] demonstrates that annexin V does not bind to viable cells. Moreover, we examined caps on RL cells induced by anti-IgM Abs, and these caps did not express annexin V binding sites. Thus, it appears that the results of Dillon et al. [18] do not apply to human B-lymphomas. Our results with anti-IgM Abs also indicate that the expression of annexin V binding sites within caps of cell surface antigens depends on the particular antigen targeted.

Apoptotic bodies are also stained by annexin V, and some photographs of budding apoptotic bodies [17] are very similar to the appearance of developing CSVs, as described in the present study as well as previously [1]. Thus, a possible relationship between the two processes should be considered. Fluorescent CSVs prepared with 1F5 are not apoptotic cells or clusters of apoptotic bodies because nuclear fragments are rarely present in CSVs prepared with 1F5. Most, although not all, apoptotic bodies contain nuclear fragments. However, fluorescent CSVs prepared with L243 generally contained nuclear fragments, and we must consider in more detail the possibility that the CSVs prepared with L243 are clusters of apoptotic bodies or apoptotic cells. There are two major factors which, when taken together, strongly suggest that production of CSVs was not a consequence of apoptosis. First, treatment of RL cells with either Ab had essentially no effect on cell viability. This is not inconsistent with the presence of nuclear



fragments in the CSVs from RL cells prepared with L243 because a few dead cells could produce a large number of such small nuclear fragments. Second, the intensity of fluorescence in the CSVs indicates that the great majority of bound Ab was delivered to CSVs. Therefore, the Abs in the CSVs must be derived primarily from viable cells.

The ability of Abs to CD20 or HLA-DR to kill cells has been tested many times. Anti-CD20 Abs were reported to induce apoptosis but, with most Abs (including 1F5), this occurred to a significant extent only if the CD20 Ab was cross-linked by a second Ab [22,23]; thus, these results are consistent with our data. The results obtained with L243 are more controversial. Nagy et al. [10,11] reported a high level of killing induced by L243 on many B-lymphoma cell lines. However, RL cells were not tested, and may be insensitive to this form of killing, considering that different cell lines varied greatly in sensitivity. Raji cells were tested by Nagy et al. [10] and were also utilized in our experiments: these were reported to be 69% killed after incubation with a saturating concentration of L243. However, we were not able to confirm these results. In our experiments, Raji cells were tightly clustered by overnight incubation with Ab at 10 – 30 µg/ml, forming large clusters of 50 or more cells which were densely packed (unpublished data). (Dense clusters of this type were not observed with RL cells.) It was impossible to disperse these clusters to obtain a viable cell count; repeated pipetting, which readily disperses normal clusters of B-lymphoma cells, was ineffective, and appeared to cause the death of many of the cells because most of the single cells released from the clusters were dead. Thus, the present studies do not support the idea that L243 induces high levels of apoptosis in Raji cells. In any case, there is less uncertainty in interpreting the results with 1F5 than the results with L243, and we believe that the CSVs prepared with L243 are basically similar to the CSVs prepared with 1F5, because they are morphologically very similar.

It is unknown whether similar events occur *in vivo*, in natural tumors or in normal lymphocytes. The results of Kennedy et al. [4], described above, suggest that this is the case in patients with CLL, but further investigations are required to decisively answer this question. It is unlikely that a new method of Ab shedding, which does not occur in some normal cells, was developed by these lymphoma cell lines. The presence of annexin V binding sites suggests that CSVs would be rapidly taken up by phagocytic cells *in vivo*, due to receptors for PS on macrophages [17], meaning that if CSVs are generated *in vivo*, they would probably have a short existence and be difficult to detect. It would be useful to investigate the interaction of CSVs with human macrophages or dendritic cells. Although Abs reactive with the cell surfaces should probably be considered a non-physiological ligand, viruses binding to cell surface receptors would induce a similar type of cross-linking, and might similarly be delivered to CSVs. Uptake of such material by macrophages or dendritic cells might have functional effects on the immune response, but such a possibility remains purely speculative at this time.

#### Acknowledgements

We are grateful to Dr David M. Goldenberg for his support.

#### References

1. Michel RB, Mattes MJ. Antibodies to CD20 and MHC class II antigen bound to B-lymphoma cells accumulate in shed cytoplasmic fragments. *Br J Cancer* 2004;91:1500–1507. [PubMed: 15452546]
2. McLaughlin P, Grillo-Lopez AJ, Link BK, Levy R, Czuczman MS, Williams ME, et al. Rituximab chimeric anti-CD20 monoclonal antibody therapy for relapsed indolent lymphoma: half of patients respond to a four-dose treatment program. *J Clin Oncol* 1998;16:2825–2833. [PubMed: 9704735]
3. Brown KS, Levitt DJ, Shannon M, Link BK. Phase II trial of Remitogen (humanized 1D10) monoclonal antibody targeting class II in patients with relapsed low-grade or follicular lymphoma. *Clin Lymphoma* 2001;2:188–190. [PubMed: 11779298]

4. Kennedy AD, Beum PV, Solga MD, DiLillo DJ, Lindorfer MA, Hess CE, et al. Rituximab infusion promotes rapid complement depletion and acute CD20 loss in chronic lymphocytic leukemia. *J Immunol* 2004;172:3280–3288. [PubMed: 14978136]
5. Söderström N. The free cytoplasmic fragments of lymphoglandular tissue (lymphoglandular bodies). *Scand J Immunol* 1968;5:138–152.
6. Ran S, He J, Huang X, Soares M, Scothorn D, Thorpe PE. Antitumor effects of a monoclonal antibody that binds anionic phospholipids on the surface of tumor blood vessels in mice. *Clin Cancer Res* 2005;11:1551–1562. [PubMed: 15746060]
7. Hansen HJ, Ong GL, Diril H, Roche PA, Griffiths GL, Goldenberg DM, et al. Internalization and catabolism of radiolabeled antibodies to the MHC class II invariant chain by B-cell lymphomas. *Biochem J* 1996;320:293–300. [PubMed: 8947500]
8. Ong GL, Mattes MJ. Processing of antibodies to the MHC class II antigen by B-cell lymphomas: release of Fab-like fragments into the medium. *Mol Immunol* 1999;36:777–788. [PubMed: 10593516]
9. Michel RB, Mattes MJ. Intracellular accumulation of the anti-CD20 antibody 1F5 in B-lymphoma cells. *Clin Cancer Res* 2002;8:2701–2713. [PubMed: 12171904]
10. Nagy ZA, Hubner B, Löhning C, Rauchenberger R, Reiffert S, Thomassen WE, et al. Fully human, HLA-DR-specific monoclonal antibodies efficiently induce programmed death of malignant lymphoid cells. *Nature Med* 2002;8:801–807. [PubMed: 12101408]
11. Nagy ZA, Mooney NA. A novel, alternative pathway of apoptosis triggered through class II major histocompatibility complex molecules. *J Mol Med* 2003;81:757–765. [PubMed: 14551703]
12. Escola JM, Kleijmeer MJ, Stoorvogel W, Griffith JM, Yoshie O, Geuze HJ. Selective enrichment of tetraspan proteins on the internal vesicles of multivesicular endosomes and on exosomes secreted by human B-lymphocytes. *J Biol Chem* 1998;273:20121–20127. [PubMed: 9685355]
13. Schreiner GF, Unanue ER. Membrane and cytoplasmic changes in B lymphocytes induced by ligand-surface immunoglobulin interaction. *Adv Immunol* 1976;24:37–165. [PubMed: 798475]
14. Loor F. Plasma membrane and cell cortex interactions in lymphocyte functions. *Adv Immunol* 1980;30:1–120. [PubMed: 7004135]
15. Pulczynski S, Boesen AM, Jensen OM. Modulation and intracellular transport of CD20 and CD21 antigens induced by B1 and B2 monoclonal antibodies in Raji and JOK-1 cells – an immunofluorescence and immunoelectron microscopy study. *Leukemia Res* 1994;18:541–552. [PubMed: 7517481]
16. Léveillé C, Reem A-D, Mourad W. CD20 is physically and functionally coupled to MHC class II and CD40 on human B cell lines. *Eur J Immunol* 1999;29:65–74. [PubMed: 9933087]
17. Verhoven B, Schlegel RA, Williamson P. Mechanisms of phosphatidylserine exposure, a phagocyte recognition signal, on apoptotic T lymphocytes. *J Exp Med* 1995;182:1597–1601. [PubMed: 7595231]
18. Dillon SR, Mancini M, Rosen A, Schlissel MS. Annexin V binds to viable B cells and colocalizes with a marker of lipid rafts upon B cell receptor activation. *J Immunol* 2000;164:1322–1332. [PubMed: 10640746]
19. Cocca BA, Cline AM, Radic MZ. Blebs and apoptotic bodies are B cell autoantigens. *J Immunol* 2002;169:159–166. [PubMed: 12077241]
20. Heijnen HFG, Schiel AE, Fijnheer R, Geuze HJ, Sixma JJ. Activated platelets release two types of membrane vesicles: microvesicles by surface shedding and exosomes derived from exocytosis of multivesicular bodies and a-granules. *Blood* 1999;94:3791–3799. [PubMed: 10572093]
21. Cardarelli PM, Quinn M, Buckman D, Fang Y, Colcher D, King DJ, et al. Binding to CD20 by anti-B1 antibody or F(ab')<sub>2</sub> is sufficient for induction of apoptosis in B-cell lines. *Cancer Immunol Immunother* 2002;51:15–24. [PubMed: 11845256]
22. Chan HT, Hughes D, French RR, Tutt AL, Walshe CA, Teeling JL, et al. CD20-induced lymphoma cell death is independent of both caspases and its redistribution into Triton-X100 insoluble membrane rafts. *Cancer Res* 2003;63:5480–5489. [PubMed: 14500384]
23. Shan D, Ledbetter JA, Press OW. Apoptosis of malignant B cells by ligation of CD20 with monoclonal antibodies. *Blood* 1998;91:1644–1652. [PubMed: 9473230]

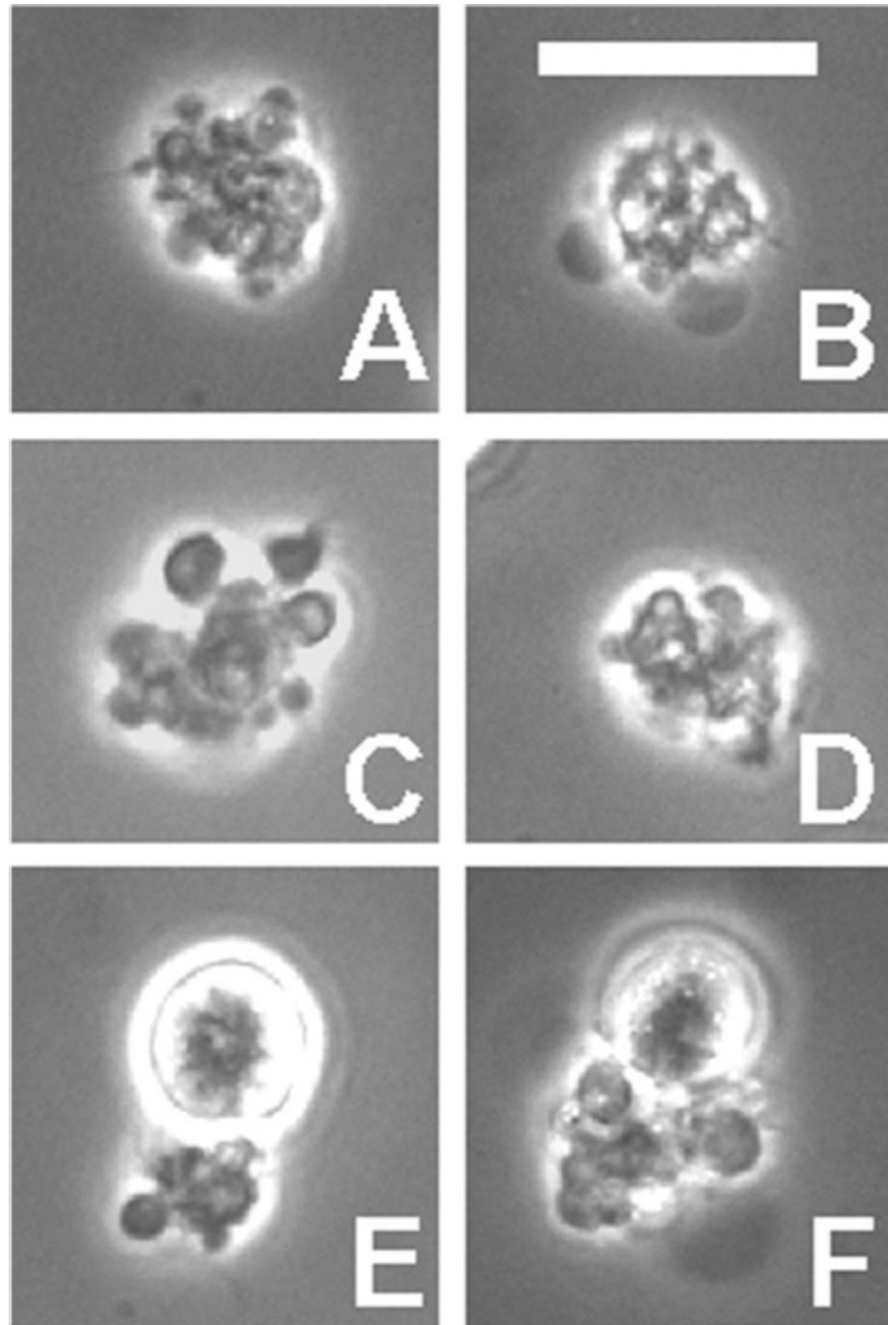


**Figure 1.**

Appearance of CSVs by phase contrast microscopy. RL cells were incubated overnight with Alexa-488-1F5, and CSVs were identified by their bright fluorescence, as also shown previously [1]. Six representative large CSVs are shown, two of which are cell bound (E and F). The size of CSVs varied greatly, and many are much smaller, but with the same complex morphology. Scale bar = 20  $\mu$ m.

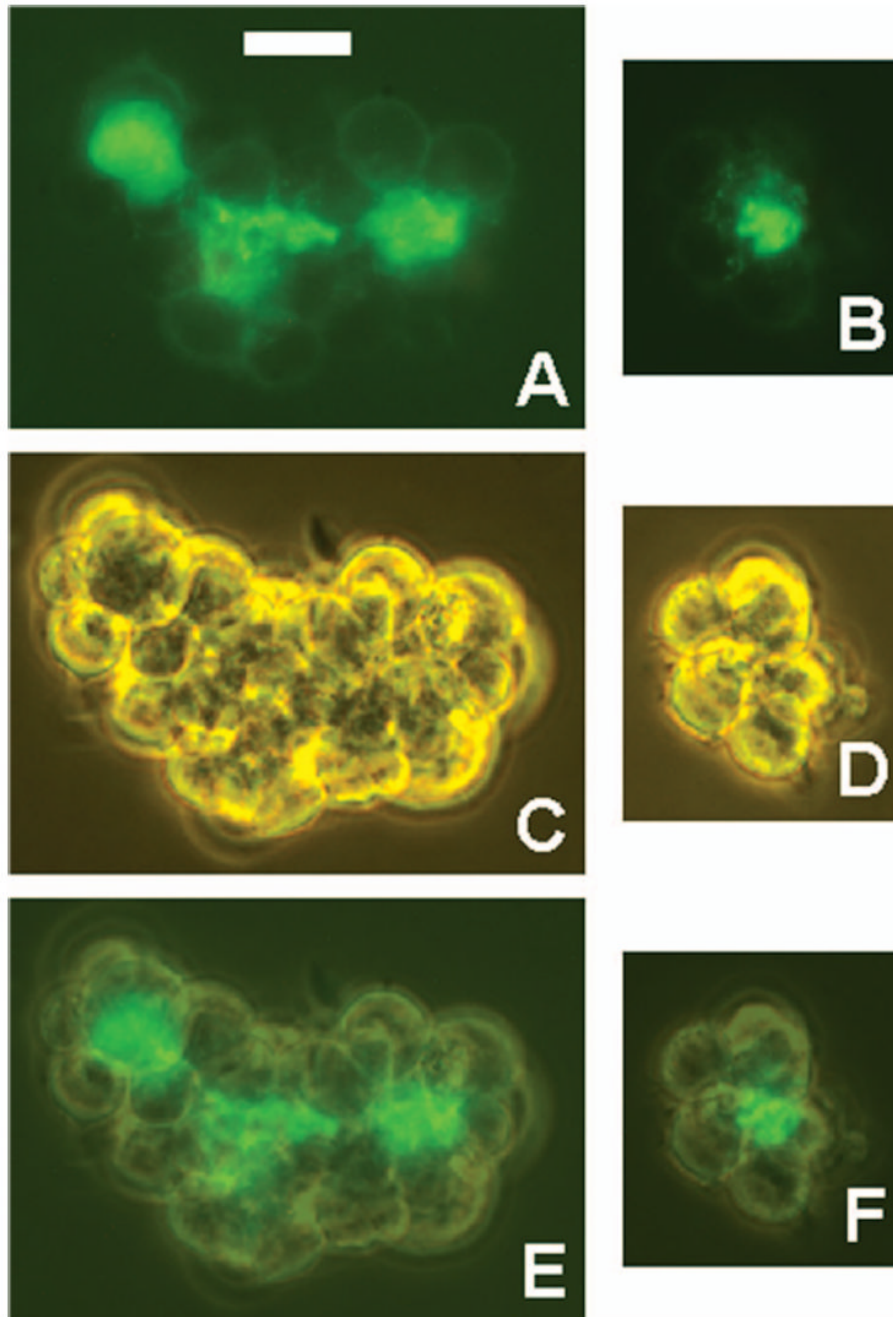


**Figure 2.** Ab L243 accumulates in the centre of cell clusters. RL cells were incubated overnight with Alexa-488-L243, and then examined without washing and without dispersing the cell clusters that had formed. Two clusters are shown by fluorescence (A,B), phase contrast (C,D) and by a mixed image of the two (E,F). Scale bar = 50  $\mu$ m.

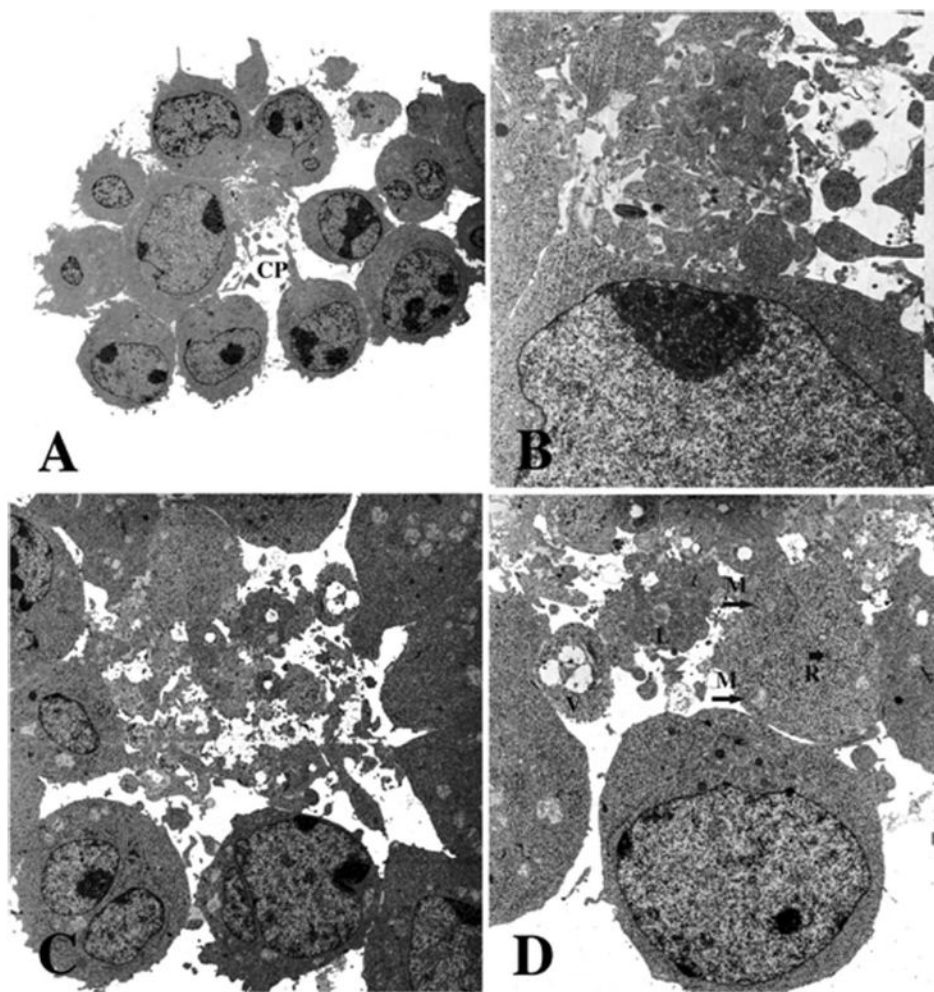


**Figure 3.** Electron microscopy of CSVs. Intact clusters that had been incubated overnight without (A,B) or with (C,D) Ab 1F5. Cells were gently fixed with glutaraldehyde, to preserve the natural clusters, and then embedded in agarose in suspension and examined by electron microscopy. The space between the cells contains a heterogeneous mass of cytoplasmic vesicles, independent of the presence of Ab. A cytoplasmic projection (CP), shown in (A), suggests a possible origin of the vesicles. The cytoplasmic fragments contain a few organelles: mitochondria (M), lipid droplets (L), vacuoles (V) and strands of RER (R) are shown (D). Magnification: (A)  $\times 7200$ ; (B)  $\times 31\,200$ ; (C)  $\times 13\,200$ ; (D)  $\times 21\,000$ . (B) is rotated  $90^\circ$  relative to (A), and (D) is rotated  $180^\circ$  relative to (C).

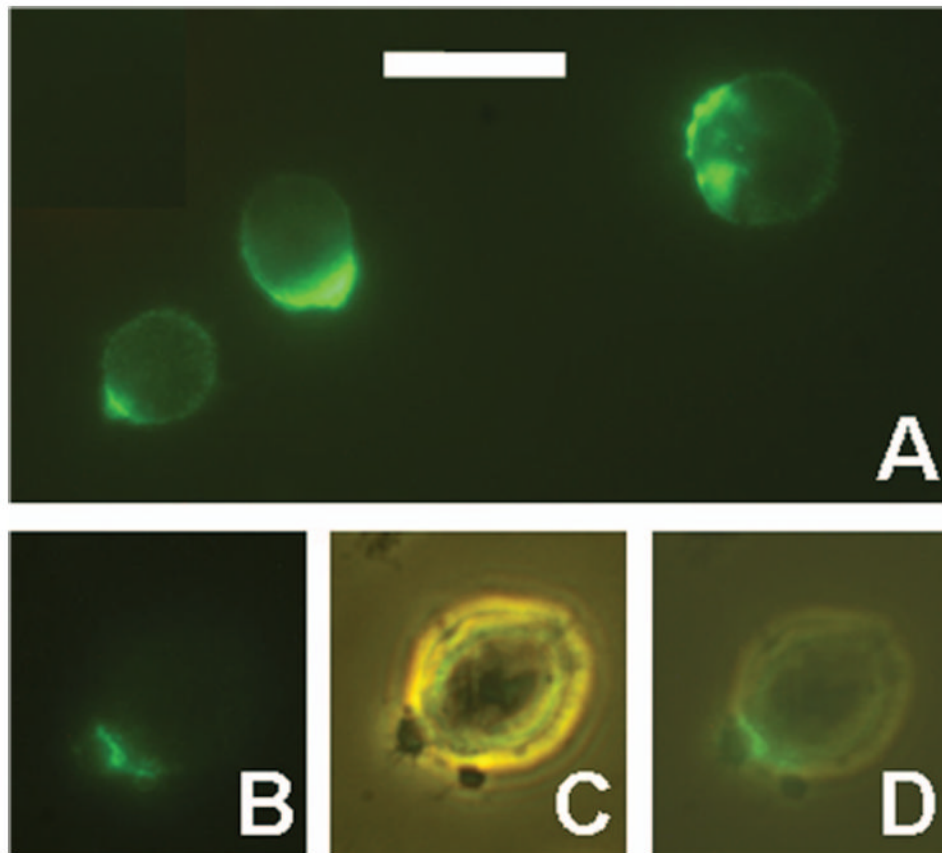


**Figure 4.** Capping of CD20 and development of small CSVs. (A) RL cells were incubated for 3 h at 37°C with Alexa-488-1F5. Various staining patterns are shown. (B–D) RL cells were incubated for 1 h at 37°C with Alexa-488-1F5, washed, and maintained at room temperature for approximately 1 h until the photographs were taken. A cell with two small blebs is shown by fluorescence (B), phase contrast (C), and a merged image of the two (D). Scale bar = 20  $\mu\text{m}$ .

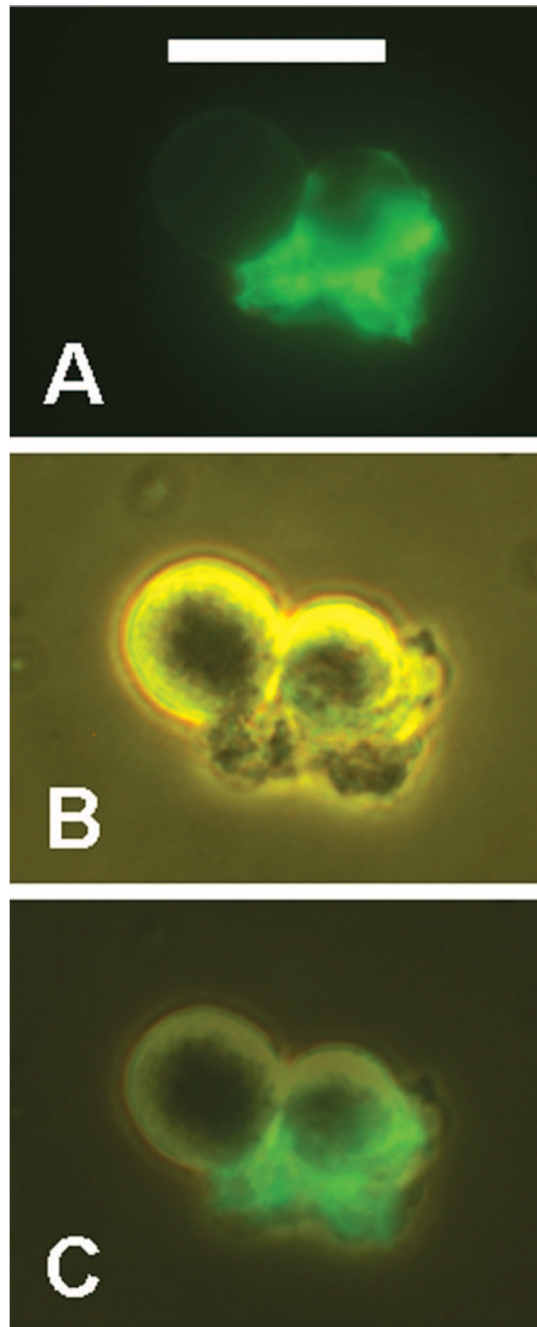


**Figure 5.** CSVs prepared with L243 (anti-HLA-DR) also contain CD20. RL cells were incubated overnight with L243, then stained for 1 h at 12°C with Alexa-488-1F5. Two clustered cells and a bound CSV are shown by fluorescence (A), phase contrast (B), and a merged image of the two (C). Scale bar = 20  $\mu\text{m}$ .

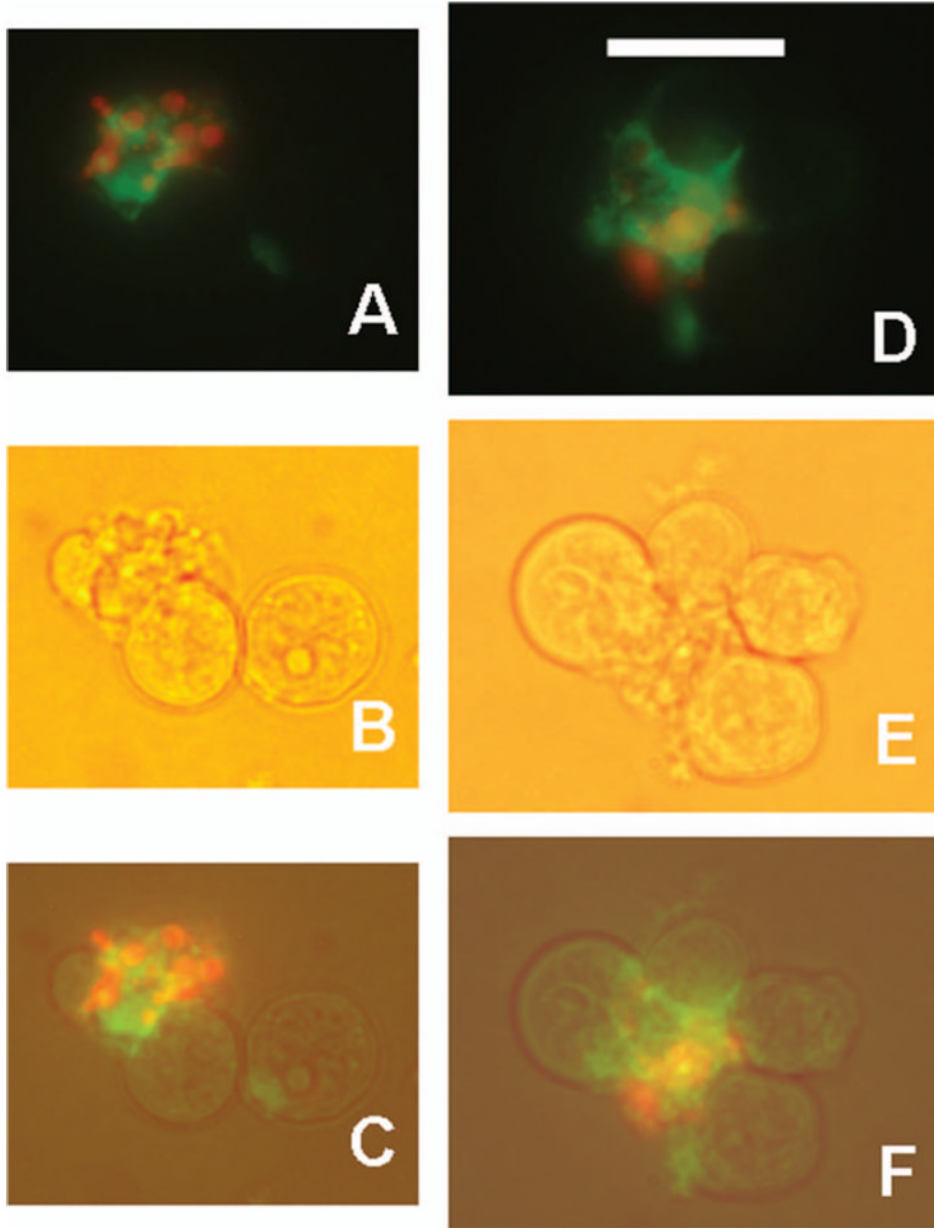


**Figure 6.**

CSVs prepared with L243 may contain nuclear fragments. RL cells were incubated overnight with L243, then stained for 1 h at 12°C with Alexa-488-1F5 (green). DNA was stained with propidium iodide (red). Two representative CSVs are shown by fluorescence only (which is a merged image of green and red exposures) (A,D), bright field light (B,E), or a merged image of the two (C,F). The objective used was a planapo  $\times 40$ , which provides brighter fluorescence than the  $\times 40$  phase contrast objective, as well as better resolution of fluorescence, which is why phase contrast was not used. Scale bar = 20  $\mu\text{m}$ .



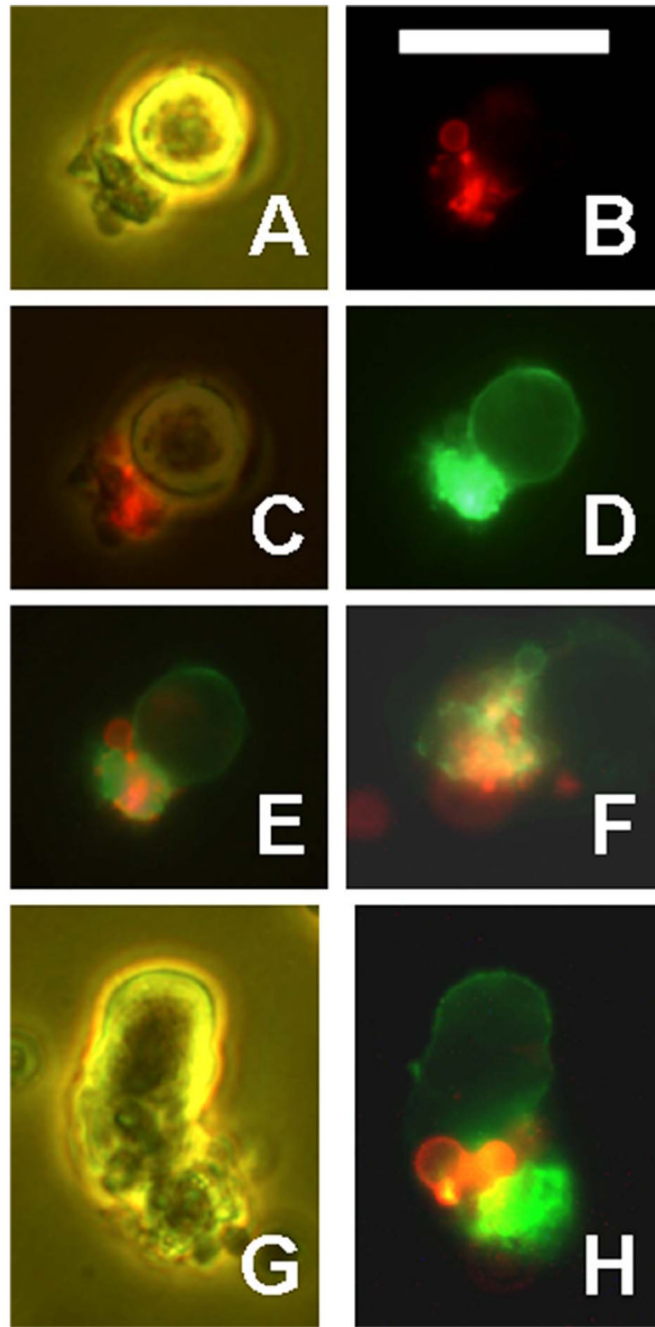


**Figure 7.** CSVs are stained by annexin V. RL cells were incubated overnight with Alexa-488-1F5 (green), then washed and stained for 45 min at room temperature with Alexa-568-annexin V (red). Representative CSVs are shown. (A – E) The same field showing phase contrast (A), red annexin V fluorescence (B), a merge of (A) and (B), green 1F5 fluorescence, overexposed to show cell surface staining (D), and a merge of red and green (E). (F) Another field showing merged red and green only. The CSV is bound to the left side of a cell which is not visible. (G – H) Another field by phase contrast (G) or by merged red and green (H). Scale bar = 20  $\mu$ m.

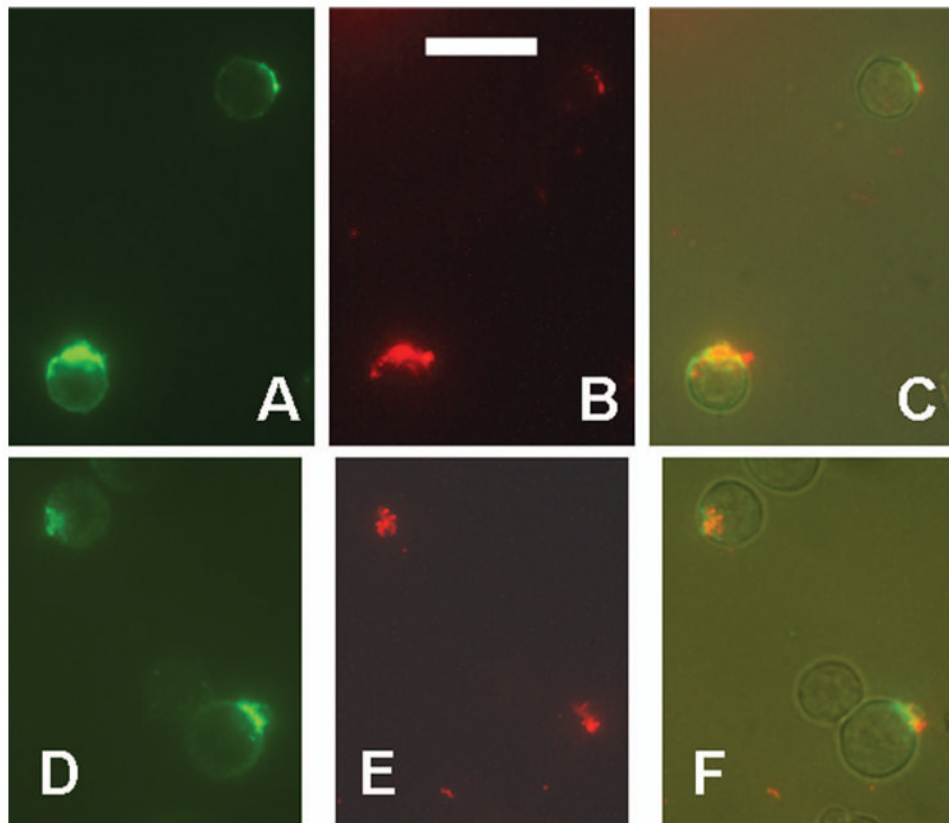


**Figure 8.**

Caps induced by anti-CD20 Abs are stained by annexin V. RL cells were incubated for 3 h at 37°C with Alexa-488-1F5 (green), and then stained for 45 min at room temperature with Alexa-568-annexin V (red). Two fields are shown. (A,D) Capped 1F5; (B,E) Annexin V staining; (C,F) a merger of three photos: green, red, and a low level of visible light, to show the cells more clearly. Scale bar = 20  $\mu$ m.

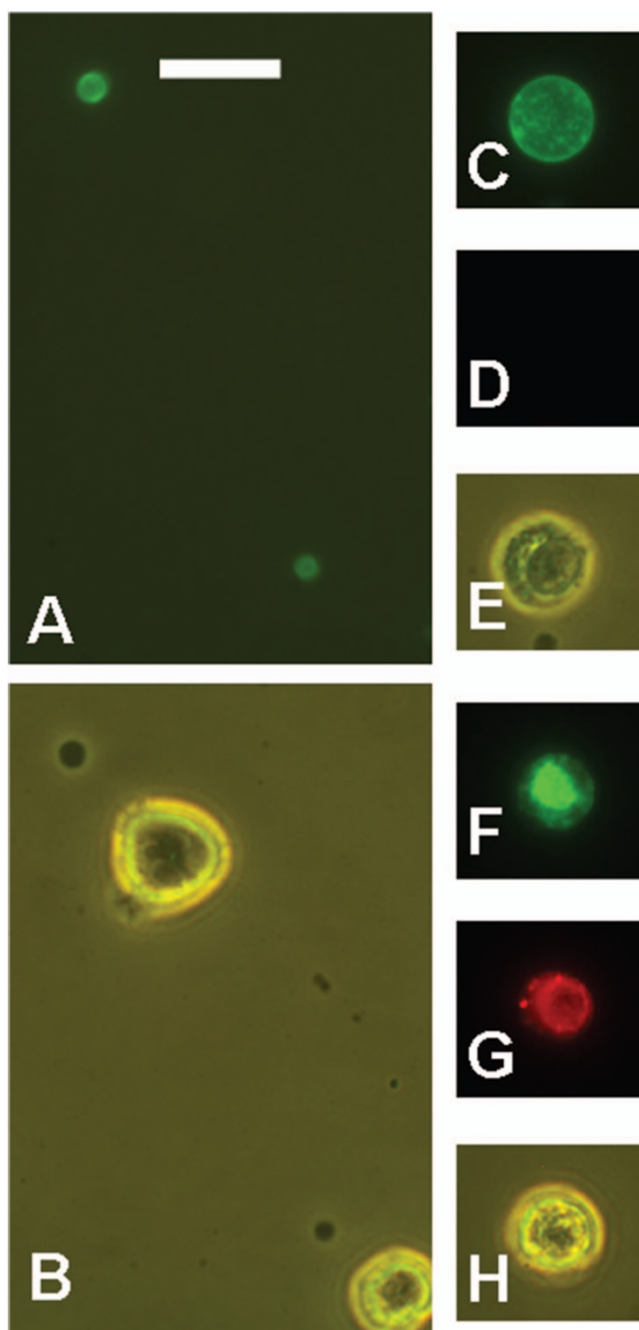


**Figure 9.** Other objects stained by Alexa-488-annexin V (green) in untreated RL cell preparations. Propidium iodide (PI) stained dead cells red. Small subcellular vesicles, shown by green fluorescence (A) or phase contrast (B). Some viable cells are shown for comparison with the size of the stained vesicles. An apoptotic cell shown by green fluorescence (C), red fluorescence (D), and phase contrast (E). The apoptotic cell did not stain with PI. A dead cell is shown by green fluorescence (F), red fluorescence (G), and phase contrast (H). Both apoptotic cells and dead cells were rare in this preparation, which was of high viability. Scale bar = 20  $\mu$ m.